Supplementary Information for

Transcutaneous co-delivery of tumor antigen and resiquimod in solid-in-oil nanodispersions promotes anti-tumor immunity

Rie Wakabayashi,[a,c] Hidetoshi Kono,[a] Shuto Kozaka,[a] Yoshiro Tahara,[a] Noriho Kamiya,[a,b,c] and Masahiro Goto*[a,b,c]

[a]Department of Applied Chemistry, Graduate School of Engineering, Kyushu University, Motooka 744, Nishi-ku, Fukuoka 819-0395, Japan.

[b]Advanced Transdermal Drug Delivery System Center, Kyushu University, Motooka 744, Nishi-ku, Fukuoka 819-0395, Japan.

[c]Center for Future Chemistry, Kyushu University, Motooka 744, Nishi-ku, Fukuoka 819-0395, Japan.

*Corresponding author. E-mail: m-goto@mail.cstm.kyushu-u.ac.jp

Table of Contents

1. Preparation of S/O nanodispersions

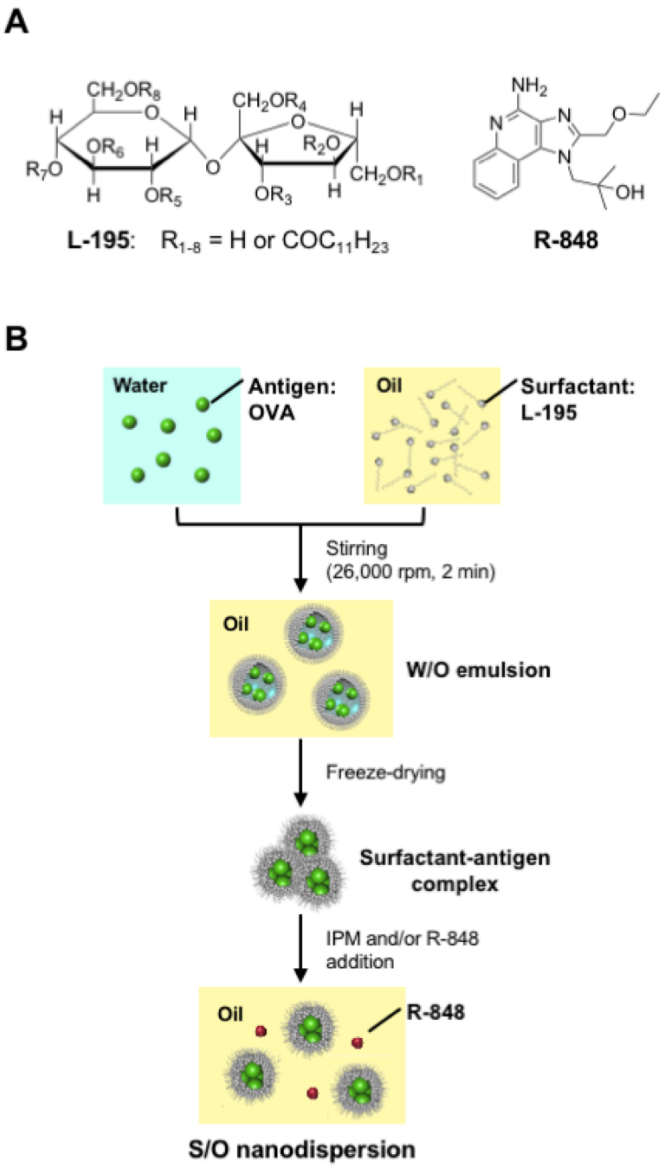

Figure S1. (A) Chemical structures of surfactant L-195 and Toll-like receptor ligand R-848 used in this study. (B) Preparation of S/O nanodispersion for co-delivery of OVA and R-848.

2. Delivery of OVA into deeper region of the skin by S/O

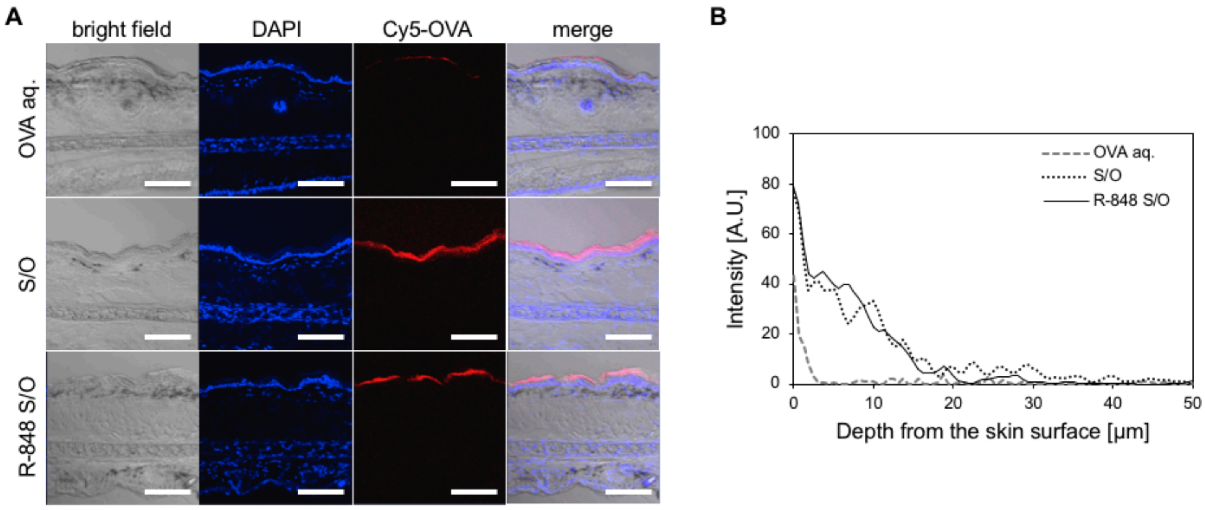

Figure S2. Transcutaneous delivery of OVA in the skin. (A) Light and fluorescence microscopy images of sections of ear auricles from C57BL/6N mice at 24 h after application of patches soaked in Cy5-OVA by PBS solution (OVA aq.), S/O nanodispersions without (S/O) or with (R-848 S/O) R-848. Skin sections were co-stained with DAPI to detect nuclei. Bars: 100 μm. (B) Skin permeation of Cy5-OVA into the deeper region of the skin.

3. Transcutaneous delivery of fluorescent dye and S/O nanoparticles

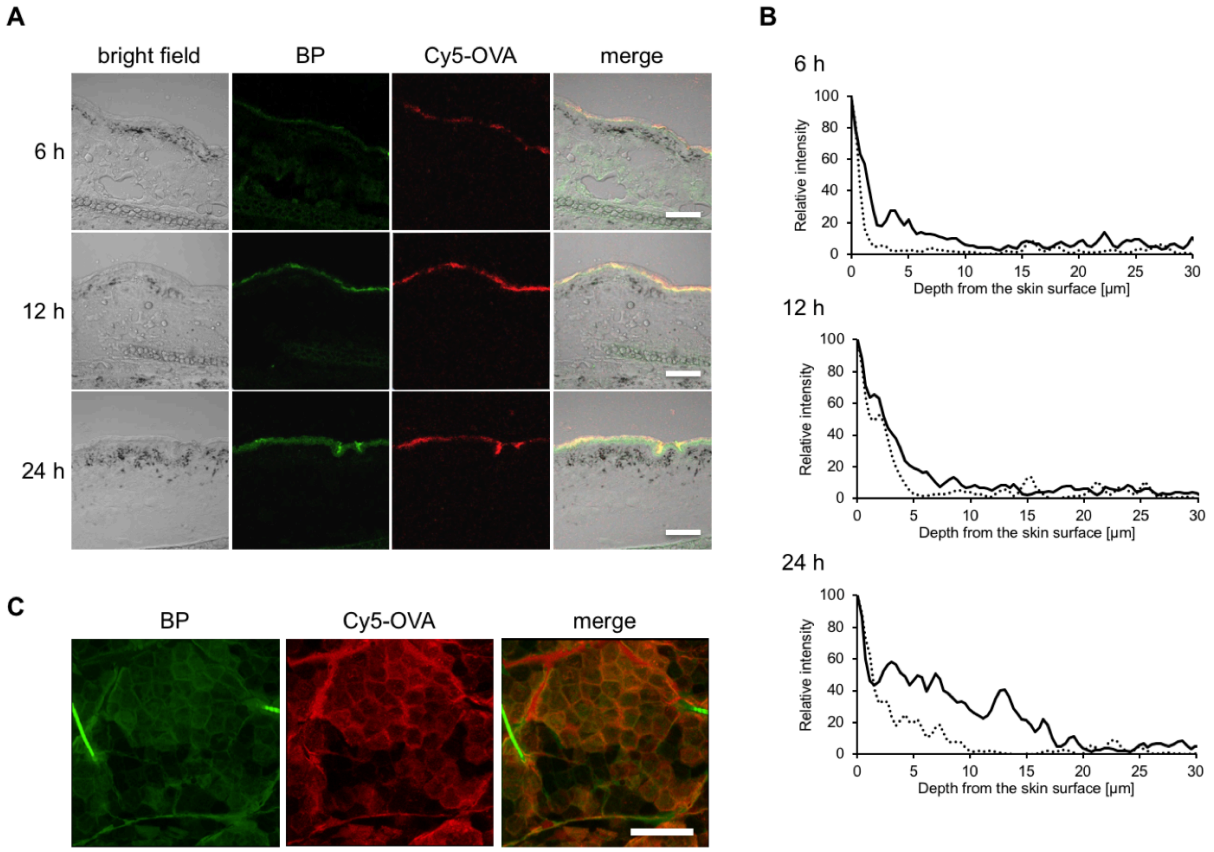

Figure S3. (A) Skin sectioning images after topical application of fluorescent dye BODIPY FL C_5 (BP) and Cy5-OVA by S/O nanodispersions. (B) Skin permeation kinetics of BP and Cy5-OVA. Solid lines: BP; dotted lines: Cy5-OVA. (C) Skin permeation pathway of BP and Cy5-OVA. Bars: 100 μm.

4. Activation of cells in the skin by transcutaneous administration of R-848 S/O nanodispersion

Patches immersed with samples (R-848, S/O, and R-848 S/O) were placed on the dorsal skin of C57BL/6N mice for 24 h. The skin was harvested and cell suspensions were prepared, which were stained with PECy7-conjugated anti-CD80 or anti-CD86 antibody (eBioscience) for flow cytometric analysis (Sony, ec800).

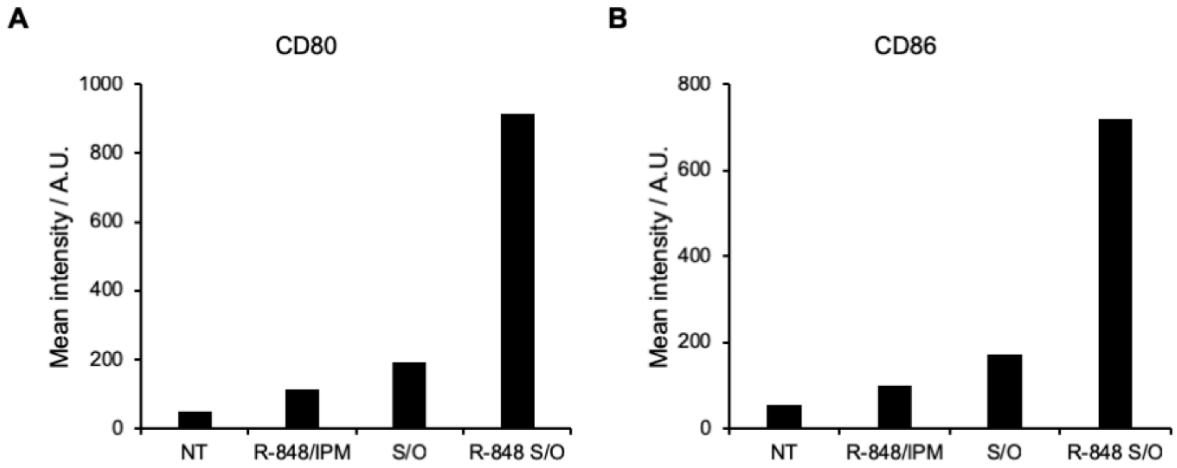

Figure S4. Activation of cells in the skin by transcutaneous administration of R-848 S/O nanodispersion. After 24 h administration, cell suspensions were prepared and stained with PECy7-conjugated anti-CD80 (A) or anti-CD86 (B) antibody.

5. Migration of skin-derived LCs holding OVA to lymph node.

Patches immersed with S/O or R-848 S/O nanodispersion were placed on the dorsal skin of C57BL/6N mice for 24 h. The patches were removed and the skin was wiped with 20% ethanol/water, and 30 μL of FITC/dibutyl phthalate (5 mg/mL):acetone = 1:1 (vol:vol) were placed at the same sites for 24 h. The mice were sacrificed, and the draining LNs were harvested. Sections of LNs (20 μm thickness) were imaged on confocal microscopy (Carl Zeiss, LSM700).

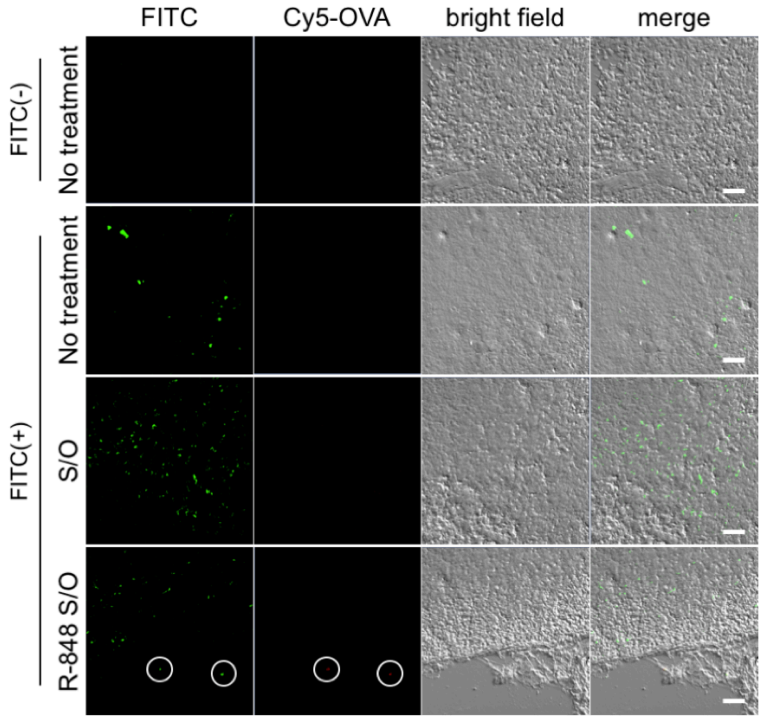

Figure S5. Migration of skin-derived DCs to lymph nodes. Fluorescence micrographs of draining lymph node sections from C57BL/6N mice after application of patches immersed with samples, followed by FITC painting to the dorsal skin. White circles indicate skin-derived LCs holding Cy5-OVA. Bars: 40 μm.

Cell suspensions of LN were analyzed by flow cytometry (Sony, ec800) to identify which subset of skin-derived DCs is holding antigens. Briefly, C57BL/6N mice were immunized as above and LNs were harvested. Cell suspensions of LNs were stained with AlexaFluoro488-anti CD207 and PECy7-anti CD103 antibodies to distinguish LCs and dermal langerin^{+} DCs as CD207^{+} CD103^{-} cells or CD207^{+} CD103^{+} cells, respectively.

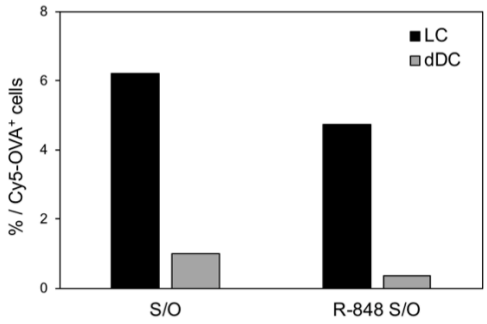

Figure S6. Percentage of LCs (CD207^{+} CD103^{-} cells) and dermal langerin^{+} DCs (CD207^{+} CD103^{-} cells) among Cy5-OVA^{+} cells in LN.

6. OVA-specific IgG production in immunized mice

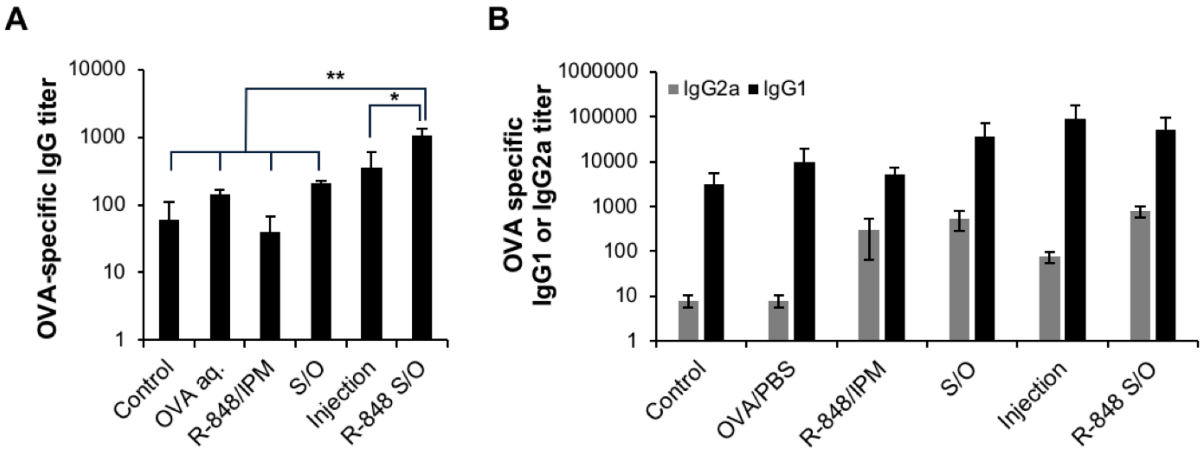

Figure S7. OVA specific total IgG titer (A) and IgG1 or IgG2a titer (B) in serum of immunized mice. N = 4, mean ± SE, $^{*}p < 0.05$, $^{**}p < 0.01$.

Table S1. Balance of OVA-specific IgG1 and IgG2a in immunized mice.

Group	**IgG1/IgG2a**
Control	386
OVA/PBS	1250
R-848/IPM	18
S/O	69
Injection	1194
R-848 S/O	66

7. Accumulation of cytotoxic T cells in the E.G7-OVA tumor

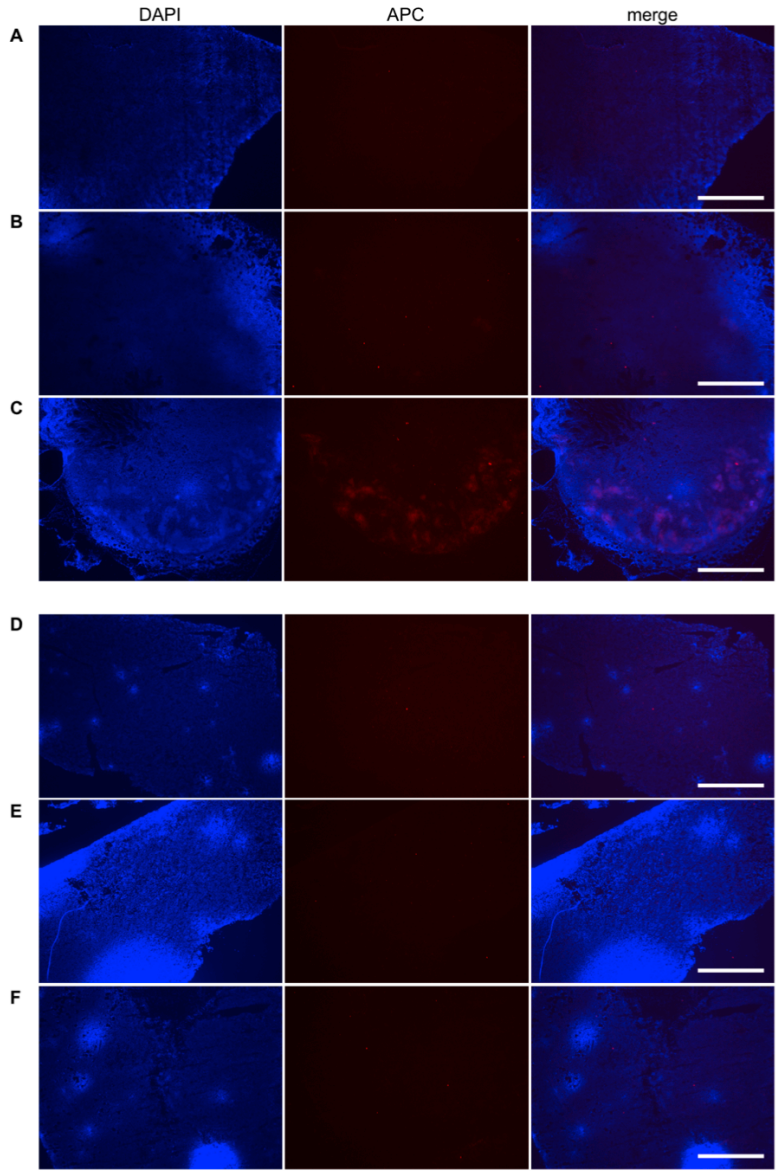

Figure S8. Accumulation of cytotoxic T cells (CTLs) at tumor site. C57BL/6N mice were immunized with s.c. injection or t.c. patch soaked with R-848 S/O nanodispersion twice and E.G7-OVA and EL4 tumor cells were inoculated. Twenty-one days after the inoculation, the tumors were harvested and sections of E.G7-OVA (A–C) or EL4 (D–F) were prepared. Sections were stained with APC-conjugated anti-CD8 to detect CTLs and DAPI to detect nuclei. Samples: (A, D) no treatment, (B, E) injection, (C, F) R-848 S/O. Bars: 1 mm.